Magnetic and superconducting properties of $FeSe_{1-x}Te_x$ ($x \sim 0$, 0.5, and 1.0)

A. V. Fedorchenko,[1] G. E. Grechnev,[1] V. A. Desnenko,[1] A. S. Panfilov,[1,a)] S. L. Gnatchenko,[1] V. V. Tsurkan,[2,3] J. Deisenhofer,[2] H.-A. Krug von Nidda,[2] A. Loidl,[2] D. A. Chareev,[4] O. S. Volkova,[5] and A. N. Vasiliev[5]

[1]*B. Verkin Institute of Low Temperature Physics and Engineering, National Academy of Sciences of Ukraine, 47 Lenin Ave., Kharkov 61103, Ukraine*

[2]*Experimental Physics 5, Center for Electronic Correlations and Magnetism, Institute of Physics, University of Augsburg, Augsburg 86159, Germany*

[3]*Institute of Applied Physics, Academy of Sciences of Moldova, MD-2028 Chisinau, Republic of Moldova*

[4]*Institute of Experimental Mineralogy, Russian Academy of Sciences, Chernogolovka, Moscow District 142432, Russia*

[5]*Moscow State University, Physics Department, Moscow 119991, Russia*

(Submitted October 12, 2010)
Fiz. Nizk. Temp. **37**, 100–107 (January 2011)

The magnetization of $FeSe_{1-x}Te_x$ ($x \sim 0$, 0.5, and 1.0) compounds has been studied in magnetic fields up to 50 kOe and at temperatures of 2–300 K. The superconducting transition was observed at $T_c \sim 8$ K and 13.6–14.2 K in $FeSe_{0.963}$ and $FeSe_{0.5}Te_{0.5}$, respectively. For most of the samples, nonlinearity of the magnetization curves in the normal state gives evidence of a common, substantial presence of ferromagnetic impurities in these compounds. By taking these impurity effects into account, the intrinsic magnetic susceptibility χ of $FeSe_{0.963}$, $FeSe_{0.5}Te_{0.5}$, and FeTe was estimated to increase gradually with Te content. For FeTe a drastic drop in $\chi(T)$ with decreasing temperature was found at $T_N \sim 70$ K, which is presumably related to antiferromagnetic ordering. To shed light on the observed magnetic properties, *ab initio* calculations of the exchange enhanced magnetic susceptibility are performed for FeSe and FeTe in the local spin density approximation. © *2011 American Institute of Physics*. [doi:10.1063/1.3552132]

I. INTRODUCTION

Following the recent discovery of the iron-pnictide high T_c superconductors (SCs),[1,2] the search for the new SCs was rapidly extended to a large variety of iron-based planar compounds.[3–8] Among them, the iron chalcogenides $FeSe_{1-x}Te_x$ are distinguished by their structural simplicity.[9] They belong to so-called "11"-type iron-based SCs and consist of iron-chalcogenide layers with square planar sheets of Fe in a tetrahedral Se (or Te) environment, maintaining the same Fe^{+2} charge state as the iron pnictides. Superconductivity with a modest transition temperature $T_c \sim 8$ K has been observed in Se deficient FeSe compounds,[9–11] whereas partial replacement of Se with Te yields $T_c \sim 15$ K at about 50% Te substitution.[12,13] However, recent reports on SC of FeSe at high pressures with $T_c \sim 27$ K,[14] 34 K,[15] 35 K,[16] and 37 K[17,18] have stimulated considerable interest in the physical properties of $FeSe_{1-x}Te_x$.

The electron-phonon interaction in the iron-based SCs is estimated to be too small to produce conventional superconductivity, and there is growing anticipation that superconductivity in the iron-based SCs is driven by spin fluctuations owing to the proximity to magnetic instability in FeSe and related compounds.[7,19,20] Itinerant spin density wave (SDW) transitions have been found in parent compounds of the Fe based SCs, which result in relatively small ordered magnetic moments, and in essentially non-Curie-Weiss behavior for the magnetic susceptibility at temperatures above T_{SDW}.[3–6] On the other hand, undoped FeTe compounds are not superconducting but magnetically ordered.[13,21,22] Moreover, the magnetic structure found in the FeTe compounds is rather different from that of parent iron-arsenide SC compounds, although similar Fermi surface nesting is predicted by DFT calculations.[7,19] It has been suggested that the electrons in the $FeTe_{1-x}Se_x$ system are localized and close to a Mott-Hubbard transition, with the local magnetic moments interacting via short-range super-exchange,[23] and that superconductivity is promoted by a combination of resonant valence bond and excitonic insulator physics.[8]

At present, there is considerable controversy regarding the interplay between electronic structure, magnetism and superconductivity in $FeSe_{1-x}Te_x$ compounds, and their complex magnetic properties are still not well characterized or understood. Experimental data on the magnetic susceptibility of $FeSe_{1-x}Te_x$ systems in the normal state are still incomplete and contradictory.[12,13,21] Also, the magnetic behavior of $FeSe_{1-x}Te_x$ systems is presumably related to the presence of magnetic impurities and secondary phases. Therefore, further studies of their magnetic and superconducting properties and the evolution of these with doping, pressure, and temperature can help in revealing the mechanism for the high-T_c superconductivity in this family of Fe-based SCs.

In order to discover the superconducting mechanism and its relation to the expected influence of spin fluctuations, it is very important to determine the intrinsic susceptibility of the Fe-based SCs. Here we report some experimental results from studies of the magnetic susceptibility of $FeSe_{1-x}Te_x$

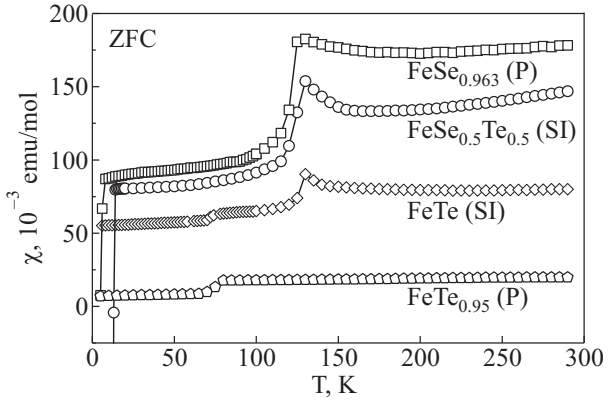

FIG. 1. Temperature dependence of the magnetic susceptibility for $FeSe_{0.963}$, $FeSe_{0.5}Te_{0.5}$, and FeTe ($FeTe_{0.95}$) measured in a magnetic field $H=200$ Oe with zero field cooling (ZFC).

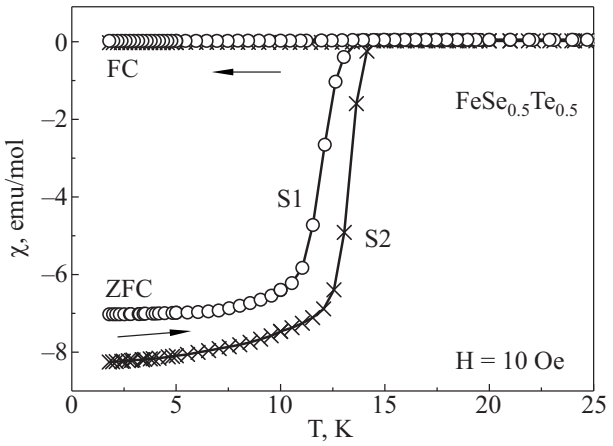

FIG. 2. Low field magnetic susceptibility in the vicinity of the superconducting transition for $FeSe_{0.5}Te_{0.5}$ single crystals of the two series S_1 and S_2.

compounds in the normal state. The main objective of this study is to discover and distinguish the magnetic properties of the parent phase from the contributions owing to secondary phases and impurities. The experiments are supplemented by *ab initio* calculations of the electronic structure and magnetic susceptibility of FeSe and FeTe within the density functional theory (DFT). Thus, the aim of this investigation is to shed more light on the relationship between the magnetic properties and the chemical and structural compositions, and also on the interplay between superconductivity and magnetic instability in $FeSe_{1-x}Te_x$ systems.

II. EXPERIMENTAL DETAILS AND RESULTS

Polycrystalline $FeSe_{0.963}$ and $FeTe_{0.95}$ samples were obtained by conventional solid-state synthesis. The starting chemicals were powder iron (Merck, 99.5%, 10 lm) and crystalline selenium and tellurium cleaned by the floating zone method. These chemicals were mixed in proportions consistent with the stoichiometry of the reaction, Fe:Se $=1:0.963$ and Fe:Te$=1:0.95$, sealed in an evacuated (10^{-4} bar) silica glass capsule, and annealed at 700 K for 14 days. The reacted mixture was ground in an agate mortar under acetone and then pressed into pellets of 6 mm in diameter under a load of 1–1.2 tons, followed by annealing in the evacuated silica glass capsule at 700 K for 20 days. Both synthesized substances were examined under a microscope in reflected light and analyzed by x-ray powder diffraction (XRD, Co K_α radiation, Fe filter) and by electron microanalysis (CAMECA SX100, 15 kV).

The single crystals with $x\sim0.5$ and 1 were grown by slow cooling by the self-flux method,[24] and two series of samples were prepared. The phase content of the samples was checked by x-ray diffraction. Here we refer to the polycrystalline and single-crystalline samples as P and S, respectively, followed by a series number. The dc magnetization studies were carried out in magnetic fields up to 50 kOe and at temperatures of 2–300 K using a superconducting quantum interference device (SQUID) magnetometer. For the single crystals, the magnetic field was applied along the tetragonal c-axis.

The temperature dependences of the magnetic susceptibility $\chi(T)$ measured in low magnetic fields (Fig. 1) exhibit few distinct features. The low temperature features are related to the superconducting transitions at $T_c\sim8$ and 13.5 K for $FeSe_{0.963}$ (P) and $FeSe_{0.5}Te_{0.5}$ (S1), respectively. Detailed data on the SC transition for the $FeSe_{0.5}Te_{0.5}$ single crystals are shown in Fig. 2. The value $T_c\sim14.2$ K obtained for the sample in the second series is close to the maximum T_c value observed at ambient pressures in the $FeSe_{1-x}Te_x$ family for $x\sim0.5$.[12,25]

Pronounced anomalies in $\chi(T)$ can be seen in Fig. 1 at 125 K. Below this temperature $\chi(T)$ exhibits a remarkable irreversibility between zero-field cooling (ZFC) and field cooling (FC, not shown in the figure) magnetization data. This may be due to the magnetite (Fe_3O_4) impurities and related to the Verwey transition, which is observed in magnetite at $T_V\sim120-125$ K.[26]

A threshold cusp in $\chi(T)$ also appears near 70 K for FeTe (S1) and $FeTe_{0.95}$ (P). According to recent neutron-scattering measurements for FeTe[21,22] this feature corresponds to an antiferromagnetic (AFM) ordering with a rather complex magnetic structure and to a simultaneous structural transition from a tetragonal lattice (at high temperatures) to a distorted orthorhombic phase.

The relatively large amount of ferromagnetic (FM) impurities in these samples is readily illustrated by the magnetization data $M(H)$ in Fig. 3. Generally, at high magnetic fields the $M(H)$ dependences show a linear behavior (dashed lines in Fig. 3) with a slope determined by the host (i.e. intrinsic) magnetic susceptibility of the sample. By extrapolating them to zero field we obtained the saturation moment values of FM impurities for our samples; these fall in the range from 25 to 300 emu/mol, and are weakly dependent on temperature.

Despite the pronounced FM impurity effects, the magnetization data shown in Fig. 3 can be used to estimate, with adequate accuracy, the host magnetic susceptibilities χ_{host} for our samples from the slope of the linear part of corresponding $M(H)$ curve at high fields. The resulting values of χ_{host} at some fixed temperatures are indicated by the solid circles in Fig. 4. In Fig. 4 we also show the detailed χ_{host} (T) data, which were obtained using the equation

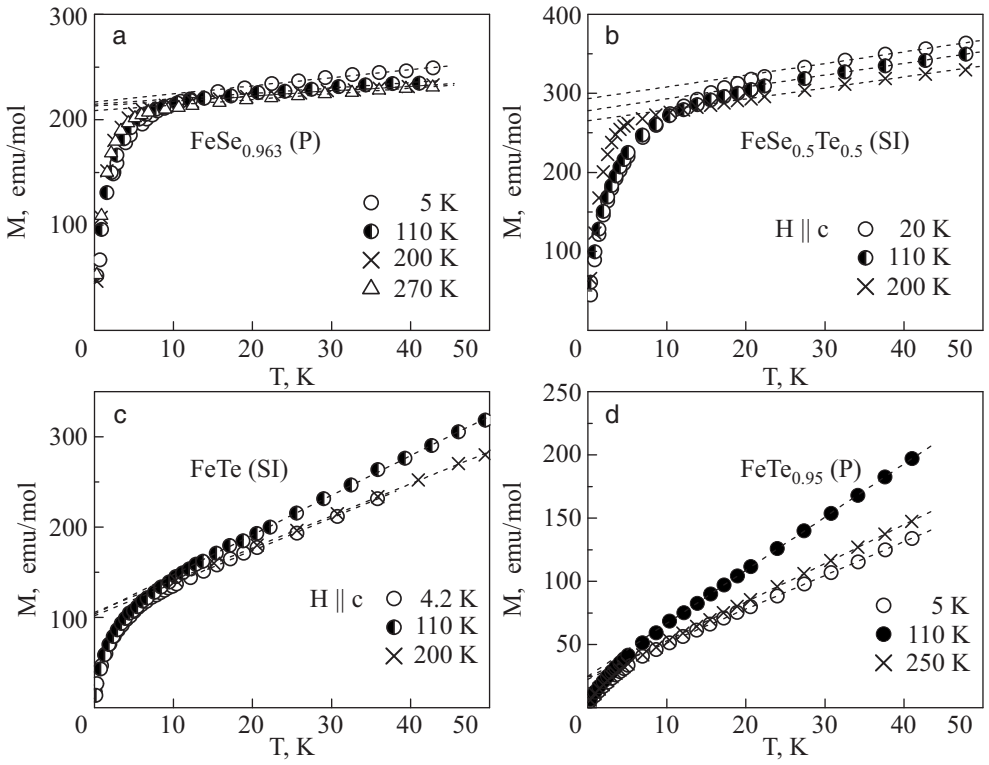

FIG. 3. Magnetization data for some $FeSe_{1-x}Te_x$ compounds at different temperatures.

$$\chi(T) \equiv \chi_{\text{host}}(T) = (M(T) - M_s)/H, \quad (1)$$

from the temperature dependence of the magnetization $M(T)$ measured in a magnetic field of 30 kOe. Here the saturation moment M_s of the FM impurity is assumed to be constant and equal to its temperature-averaged value for a given sample.

Figure 5 shows the magnetization data at selected temperatures for $FeSe_{0.5}Te_{0.5}$ and FeTe single crystals of the second series. Compared to the first series (see Fig. 3b), the $FeSe_{0.5}Te_{0.5}$ sample appeared to have a much lower saturation moment for the FM impurities. In addition, the temperature dependence of its host magnetic susceptibility (inset in

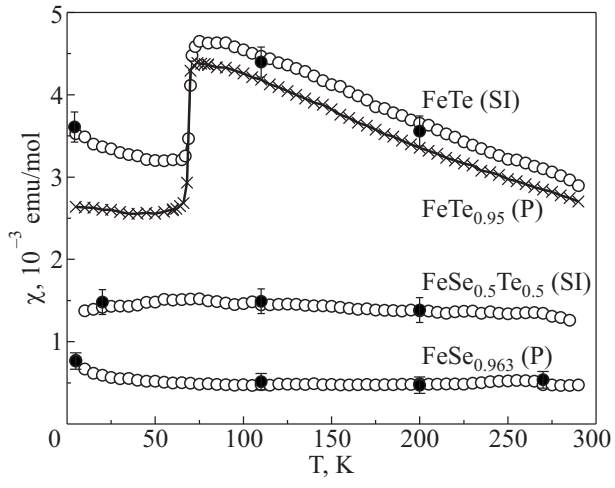

FIG. 4. Temperature dependence of the host magnetic susceptibility for some $FeSe_{1-x}Te_x$ compounds. The solid circles correspond to values derived from the high field magnetization data in Fig. 3.

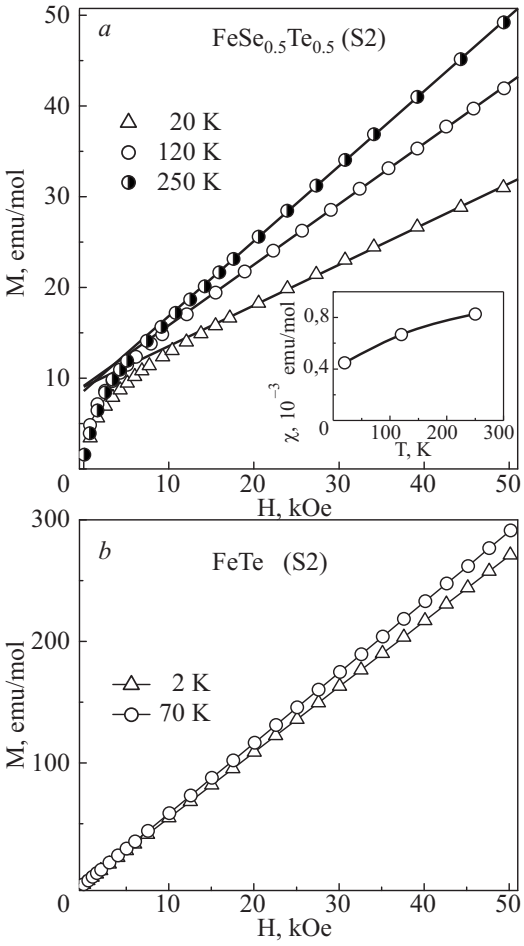

FIG. 5. Magnetization data for $FeSe_{0.5}Te_{0.5}$ (*a*) and FeTe (*b*) single crystals of the second series (S2) at different temperatures. In inset are the values of the host magnetic susceptibility versus temperature for $FeSe_{0.5}Te_{0.5}$, derived from its high field magnetization data.

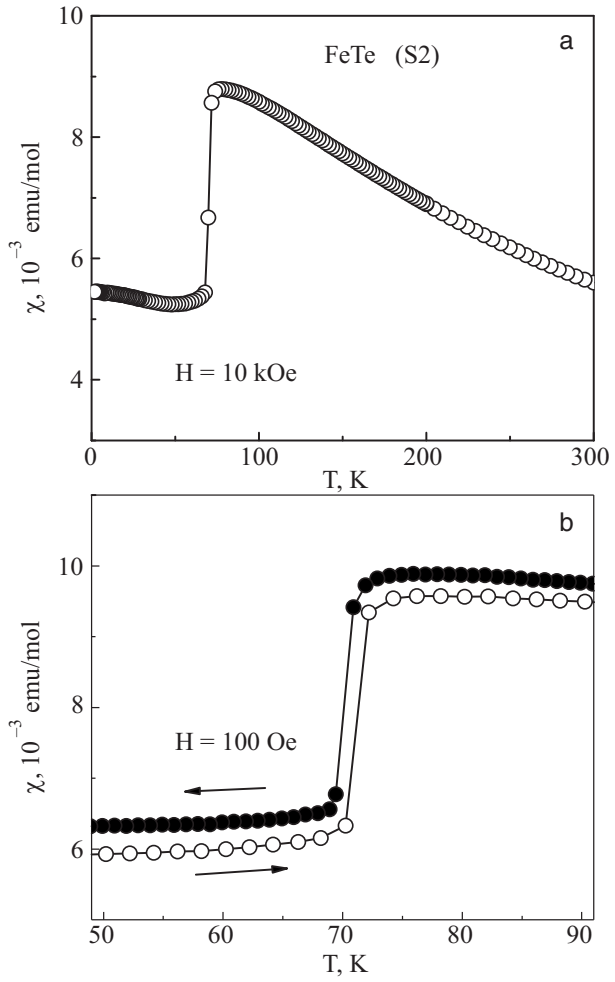

FIG. 6. Temperature dependence of the magnetic susceptibility for FeTe (S2) single crystal (*a*) and its hysteresis behavior (*b*) in vicinity of the phase transition at $T \sim 70$ K.

Fig. 5a) is distinctly different from that of the first series sample (Fig. 4), both in the character and in the magnitude of the susceptibilities. As the linear $M(H)$ dependence for FeTe in Fig. 5b implies, there are no detectable FM impurities in this sample. The temperature dependence of its magnetic susceptibility shown in Fig. 6a exhibits almost the same behavior in the vicinity of the phase transition as does $\chi(T)$ for the polycrystalline $FeTe_{0.95}$ sample and the FeTe single crystal from the first series (Fig. 4) but effect is more pronounced in magnitude. A small hysteresis in the $\chi(T)$ curve is observed after heating the sample to about 200 K with subsequent cooling to below the transition temperature (Fig. 6b). Similar behavior of $\chi(T)$ for FeTe was also reported in Ref. 22.

The basic experimental superconducting and magnetic characteristics of the samples are summarized in Table I.

TABLE I. Superconducting transition temperature T_c (K), FM impurity saturation magnetic moment M_s (emu/mol) and host (intrinsic) magnetic susceptibility χ (10^{-3} emu/mol) at room and zero temperature for $FeTe_{1-x}Se_x$ compounds.

Compound	T_c	M_s	χ	
			290 K	0 K
$FeSe_{0.963}$ (P)	~7	214	0.5 ± 0.1	0.75 ± 0.1
$FeSe_{0.5}Te_{0.5}$ (S1)	13.5	280	1.3 ± 0.2	1.45 ± 0.2
$FeSe_{0.5}Te_{0.5}$ (S2)	14.2	9	0.85 ± 0.1	0.4 ± 0.1
$FeTe_{0.95}$ (P)	—	24	2.7 ± 0.2	2.65 ± 0.2
FeTe (S1)	—	103	2.9 ± 0.2	3.6 ± 0.2
FeTe (S2)	—	~0	5.7 ± 0.2	5.45 ± 0.2

III. COMPUTATIONAL DETAILS AND RESULTS

To gain further insight into the magnetic properties of the $FeSe_{1-x}Te_x$ system in the normal state, *ab initio* calculations of the electronic structure and exchange-enhanced magnetic susceptibility were performed for the FeSe and FeTe parent compounds using the DFT and the local spin density approximation.

Under ambient conditions, the $FeSe_{1-x}Te_x$ compounds have a tetragonal PbO-type crystal structure (space group $P4/nmm$), which exhibits strong two-dimensional features. The crystal lattice is composed of alternating triple-layer slabs, which are stacked along the *c*-axis. Each iron layer is sandwiched between two nearest-neighbor chalcogen layers, which form edge-shared tetrahedrons around the iron sites. The positions of the Se (or Te) sheets are fixed by the internal parameter *Z*, which represents the height of the chalcogen atoms above the iron square plane. This parameter also determines the chalcogen-Fe bond angles. The crystal structure parameters of $FeSe_{1-x}Te_x$ compounds have been found by x-ray and neutron diffraction studies.[11,13,14,21,22]

Previous *ab initio* calculations of the electronic structure of the "11"-type iron-based chalcogenides were predominantly related to studies of AFM and SDW ordering.[19,20,23,31–34] In this paper the electronic structure calculations are carried out for FeSe and FeTe compounds with the aim of examining the paramagnetic response in an external magnetic field, and of elucidating the nature of the paramagnetism and magnetic instability in the parent phases of "11" systems. The *ab initio* calculations are carried out using the full-potential all-electron relativistic linear muffin-tin orbital method (FP-LMTO, code RSPt[35,36]). No shape approximations were imposed on the charge density or potential; this is especially important for anisotropic, layered crystal structures. The exchange-correlation potential was treated within the local spin density approximation (LSDA,[37]) of the density functional theory. Experimental lattice parameters from Refs. 10, 11, 13, 14, 21, and 22 were used in the calculations.

The basic features of the calculated electronic structure of FeSe and FeTe are in qualitative agreement with earlier results.[19] In particular, the detailed density of states (DOS) $N(E)$ of FeSe is shown in Fig. 7. In the vicinity of the Fermi level E_F the *d*-states of Fe provide the dominant contribution to the DOS in the range from −2 eV to 2 eV around E_F=0. The *p*-states of the chalcogen atoms are predominantly extended in the interstitial region, and their partial contributions to the DOS in the vicinity of E_F are substantially smaller for both FeSe and FeTe. As seen in Fig. 7, in FeSe the Fermi level lies at the steep slope of $N(E)$, at the beginning of a pseudogap of ~0.7 eV. In fact, there is a van Hove singularity in $N(E)$ at about 0.05 eV below E_F (see Fig. 6). The calculated $N(E_F)$ for FeSe can be related to the measured electronic specific heat coefficient, γ=9.17 mJ/mol

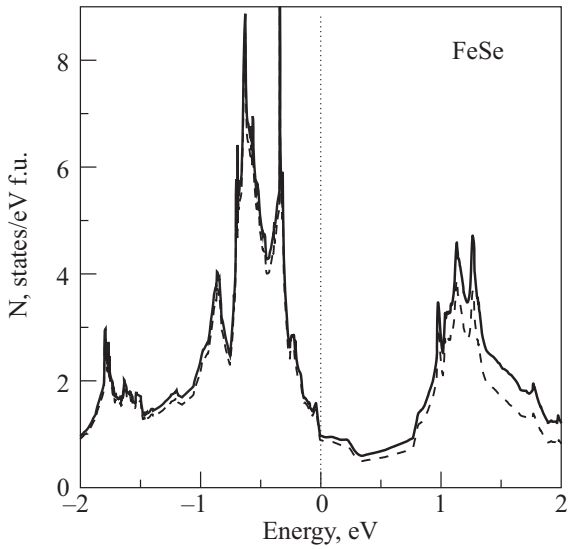

FIG. 7. Total density of states of the paramagnetic FeSe around *EF* (solid line) and the partial contribution of the iron *d*-states (dashed line). The Fermi level position (at 0 eV) is marked by a vertical line.

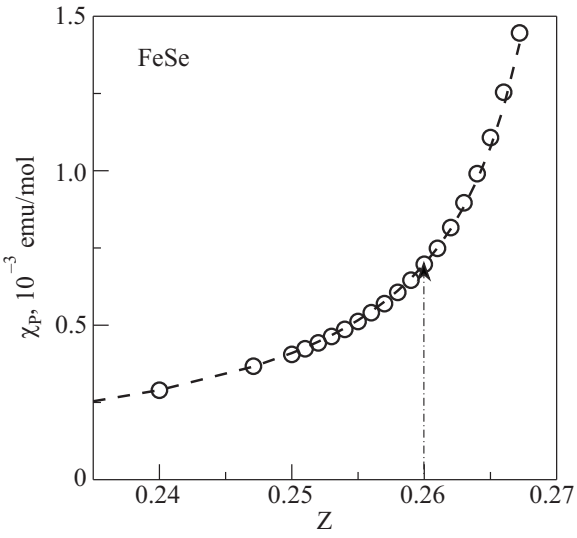

FIG. 8. Calculated paramagnetic susceptibility of FeSe as a function of the internal lattice parameter *Z*. The unit cell volume and c/a ratio are fixed to their experimental ambient pressure values (78.4 Å^3 and 1.464[14]). The dashed line is a guide for the eye. The dashed-dotted line corresponds to the experimental *Z*.

K2[9] through the Sommerfeld coefficient $\gamma = 2\pi^2 k_B^2 N(E_F)(1+\lambda)/3$. This yields an estimate for the enhancement factor in FeSe: $\lambda = 3.8$. Also, the derivatives $d \ln N(E_F)/d \ln V$ for bulk FeSe and FeTe are found to be positive and equal to 1.25 and 1.42, respectively, which suggests a reduction in $N(E_F)$ with pressure.

Self-consistent FP-LMTO-LSDA calculations of the field-induced spin and orbital (Van Vleck) magnetic moments were carried out for FeSe and FeTe through the procedure described in Ref. 36 by means of the Zeeman operator

$$\mathcal{H}_Z = \mu_B \mathbf{H}(2\hat{\mathbf{s}} + \hat{\mathbf{l}}), \tag{2}$$

which was incorporated in the original FP-LMTO Hamiltonian. Here $\mathbf{H}$ is the external magnetic field, and $\hat{\mathbf{s}}$ and $\hat{\mathbf{l}}$ are the spin and orbital angular momentum operators, respectively. The field induced spin and orbital magnetic moments were calculated for an external field of 10 T and yielded estimates of the related contributions to the magnetic susceptibility, χ_{spin} and χ_{orb}.

The paramagnetic contributions χ_{spin} and χ_{orb} for the tetragonal crystal structure of FeSe were derived from the magnetic moments for external fields parallel and perpendicular to the *c* axis. The resulting magnetic anisotropy, which is determined by the orbital contribution, appeared to be negligible, in comparison with the dominant χ_{spin} contribution. The orbital Van Vleck contribution itself is substantially smaller than the strongly enhanced spin susceptibility, and comes from the *d*-states of Fe.

In the course of the calculations, we found that magnetic response to the external field is very sensitive to the height *Z* of the chalcogen species above the Fe plane. The corresponding calculated variations in the magnetic susceptibility of FeSe and FeTe are plotted in Figs. 8 and 9, respectively. It should be noted here that the itinerant nature of the hybridized 3*d*-states of Fe is an essential condition for the above-described field-induced calculations of the paramagnetic susceptibility. There is strong experimental support for this itinerant picture for FeSe, which is expected to be in a non-magnetic spin-degenerate state. For FeTe, however, the validity of the calculated field-induced χ is questionable because of the expected more localized nature of the 3*d*-states. For this reason, the calculations for FeTe were done only for volumes smaller than the experimental volume, and these results have to be thoroughly verified by other methods, and compared with experimental data.

The enhanced Pauli spin contribution to the magnetic susceptibility was also calculated within the Stoner model

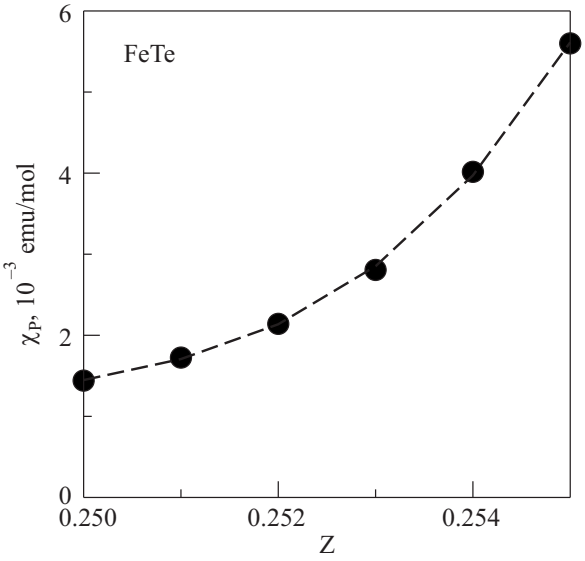

FIG. 9. Calculated paramagnetic susceptibility of FeTe as a function of the internal lattice parameter *Z* for LSDA optimized (87 Å^3) unit cell volume. The c/a ratio is fixed to the experimental ambient pressure value (1.647[14]). The dashed line is a guide for the eye.

$$\chi_{\text{ston}} = S\chi_P \equiv \mu_B^2 N(E_F)[1 - IN(E_F)]^{-1}, \quad (3)$$

where $\chi_P = \mu_B^2 N(E_F)$, S is the Stoner enhancement factor, and μ_B is the Bohr magneton. The multi-band Stoner integral I, representing the exchange-correlation interactions for conduction electrons and appropriate for these compounds, can be expressed in terms of the calculated parameters of the electronic structure[38] as

$$I = 1/N(E_F)^2 \sum_{qll'} N_{ql}(E_F) J_{qll'} N_{ql'}(E_F). \quad (4)$$

Here $N(E_F)$ and $N_{ql}(E_F)$ are the total density of electronic states and the projected DOS at site q and angular momentum l on the Fermi level. The parameters of the exchange interaction $J_{qll'}$ are defined in terms of the intra-atomic exchange integrals,

$$J_{qll'} = \int g(\rho(r))\phi_{ql}(r)^2 \phi_{ql'}(r)^2 dr, \quad (5)$$

and, therefore, depend upon the corresponding partial wave functions $\phi_l(r)$. Here $g(\rho(r))$ is a function of the electron density,[37] and l and l' are the corresponding angular momentum quantum numbers.

In the framework of an itinerant model of magnetism, the mean field treatment within the Stoner model can be valid at least to establish trends. This model predicts that the FeTe system will be unstable in a non-magnetic state. For FeSe the calculated value of the enhanced Pauli susceptibility ($\chi_{\text{ston}} \sim 0.4 \cdot 10^{-3}$ emu/mol) is close to the calculated field-induced χ_{spin} for the same range of lattice parameters. The calculated susceptibility enhancement factor S appears to be about 10, and this means proximity to a quantum critical point in the pure FeSe compound with possible competition between FM and AFM spin fluctuations.

IV. DISCUSSION

The experimental superconducting and magnetic characteristics obtained for $FeSe_{1-x}Te_x$ compounds studied here are in reasonable agreement with those reported in Refs. 13, 22, and 27–30. In particular, the intrinsic magnetic susceptibility derived here for the normal state of $FeSe_{0.963}$ is close to that cited recently in Ref. 27 for polycrystalline $Fe_{1.11}Se$. The inherent feature of the FeSe–FeTe system revealed in our study is a high sensitivity of the magnetic properties to the quality and composition of the samples. This can be readily demonstrated using the data for $FeSe_{0.5}Te_{0.5}$ and FeTe compounds listed in Table I. Despite an appreciable uncertainty, the experimental data suggest a gradual increase in the magnetic susceptibility of $FeSe_{1-x}Te_x$ systems with increasing amounts of tellurium.

In comparing the experimental data on χ from Table I with the calculations of Fig. 8 we note that the experimental internal lattice parameter Z in FeSe is about 0.26,[10,11,14] whereas the optimized DFT calculated values of Z are 0.234[19] and 0.26.[33] Though the calculated paramagnetic susceptibility is very sensitive to the height Z of Se atoms above the Fe plane, we can estimate the corresponding contributions to χ as $\chi_{\text{spin}} = 0.55 \cdot 10^{-3}$ emu/mol and $\chi_{\text{orb}} = 0.11 \cdot 10^{-3}$ emu/mol for the experimental lattice parameters of FeSe ($V = 78.4$ Å^3, $c/a = 1.464$, $Z = 0.26$[14]). Therefore, the calculated field-induced magnetic moments are in qualitative agreement with the experimentally measured susceptibility of FeSe in the paramagnetic region (Table I). Actually, the FeSe compound is found to be on the verge of magnetic instability. The proximity to a quantum critical point can be seen clearly in Fig. 8, and this nearness can result in strong spin fluctuations.

For FeTe the Stoner criterion is fulfilled for the experimental values of the cell volume and the parameter Z. Actually, our self-consistent field-induced LSDA calculations for FeTe converged to the paramagnetic state only for reduced lattice parameters. This is especially relevant to the parameter Z, which also had to be reduced by about 10%. Therefore, we should regard the calculated paramagnetic susceptibility of FeTe in Fig. 9 as a rough estimate which may be valid at least to establish a trend in the effect of the parameter Z. A detailed study of pressure effects on χ is highly desirable in order to address further the extent to which a qualitative agreement between the calculated χ and experimental data for FeTe in Table I might merely be fortuitous.

A detailed investigation of $\chi(T)$ and $\chi(x)$ in $FeSe_{1-x}Te_x$ compounds merits a separate investigation beyond the scope of this study. In order to elucidate in a systematic way the effects of isovalent partial substitution of Te for Se in the system, an extended concentration range must be examined. Also, further improvements in the technology for preparing the samples are to be desired. On the theoretical side, a more rigorous computational technique for FeTe and the alloys is needed, presumably employing the so-called disordered local moments (DLM) approach,[34,39] which seems relevant for the localized states of Fe.

V. CONCLUSIONS

The magnetic susceptibility of $FeSe_{1-x}Te_x$ ($x \sim 0$, 0.5, and 1.0) compounds has been investigated in the temperature range 2–300 K. Superconducting transitions are detected at 8 K and 13.6–14.2 K in $FeSe_{0.963}$ and $FeSe_{0.5}Te_{0.5}$ samples, respectively. For most of the samples, nonlinearity in the magnetization curves in the normal state indicates a substantial content of ferromagnetic impurities. By taking these impurity effects into account, the intrinsic magnetic susceptibility χ in the series of iron chalcogenides $FeSe_{0.963}$, $FeSe_{0.5}Te_{0.5}$ and FeTe was estimated to increase gradually with Te content by about a factor of 10.

Ab initio calculations of the electronic structure and paramagnetic contributions to the susceptibility of the FeSe compounds have revealed that this system is in close proximity to a quantum critical point, and this nearness can result in strong spin fluctuations. The calculated paramagnetic susceptibility in external magnetic fields appears to be close to the experimental value. The Van Vleck contribution to χ in FeSe, which amounts to as much as 20% of the total susceptibility, comes mainly from d-electrons of Fe, and should not be neglected in comparisons with the experimental data. In general, the numerical results indicate that the itinerant magnetism theory is of relevance for describing the magnetic properties of the FeSe system.

For FeTe a drastic drop in $\chi(T)$ with decreasing temperature was found at $T_N \sim 70$ K, which is presumably related to antiferromagnetic ordering. The LSDA calculated paramag-

netic susceptibility (Fig. 9), which is of the same order as the experimental data, reveals a drastic sensitivity to the structural parameter Z. Therefore, a detailed study of the effect of pressure on χ would be very useful to further address the question of the nature of the paramagnetic state in FeTe. There is also a need for rigorous calculations of χ for FeTe, which should take disorder in the local magnetic moments above T_N into account. In particular, a recent employed *ab initio* DLM approach[34,39] seems very promising as a means of shedding light on behavior of $\chi(T,P)$.

We dedicate this paper to the 100th anniversary of the birth of David Shoenberg, who was a pioneer of low temperature physics and of research on the electronic structure of solids.

This work has been supported by the Russian-Ukrainian RFBR-NASU project 43-02-10 and 10-02-90409.

[a)]Email: panfilov@ilt.kharkov.ua

[1]H. Takahashi, K. Igawa, K. Arii, Y. Kamihara, M. Hirano, and H. Hosono, Nature **453**, 376 (2008).
[2]Z.-A. Ren, W. Lu, J. Yang, W. Yi, X.-L. Shen, Z.-C. Li, G.-C. Che, X.-L. Dong, L.-L. Sun, F. Zhou, and Z.-X. Zhao, Chin. Phys. Lett. **25**, 2215 (2008).
[3]Yu. A. Izyumov and E. Z. Kurmaev, Phys. Usp. **51**, 1261 (2008).
[4]A. L. Ivanovskii, Phys. Usp. **51**, 1201 (2008).
[5]M. V. Sadovskii, Phys. Usp. **51**, 1229 (2008).
[6]K. Ishida, Y. Nakai, and H. Hosono, J. Phys. Soc. Jpn. **78**, 062001 (2009).
[7]D. J. Singh, Physica C **469**, 418 (2009).
[8]J. A. Wilson, J. Phys.: Condens. Matter **22**, 203201 (2010).
[9]F. C. Hsu, J. Y. Luo, K. W. Yeh, T. K. Chen, T. W. Huang, P. M. Wu, Y. C. Lee, Y. L. Huang, Y. Y. Chu, D. C. Yan, and M. K. Wu, Proc. Natl. Acad. Sci. U.S.A. **38**, 14262 (2008).
[10]T. M. McQueen, Q. Huang, V. Ksenofontov, C. Felser, Q. Xu, H. Zandbergen, Y. S. Hor, J. Allred, A. J. Williams, D. Qu, J. Checkelsky, N. P. Ong, and R. J. Cava, Phys. Rev. B **79**, 014522 (2009).
[11]E. Pomjakushina, K. Conder, V. Pomjakushin, M. Bendele, and R. Khasanov, Phys. Rev. B **80**, 024517 (2009).
[12]K.-W. Yeh, T.-W. Huang, Y.-L. Huang, T.-K. Chen, F.-C. Hsu, P. M. Wu, Y.-C. Lee, Y.-Y. Chu, C.-L. Chen, J.-Y. Luo, D. C. Yan, and M. K. Wu, Europhys. Lett. **84**, 37002 (2008).
[13]B. C. Sales, A. S. Sefat, M. A. McGuire, R. Jin, D. Mandrus, and Y. Mozharivskyj, Phys. Rev. B **79**, 094521 (2009).
[14]Y. Mizuguchi, F. Tomioka, S. Tsuda, T. Yamaguchi, and Y. Takano, Appl. Phys. Lett. **93**, 152505 (2008).
[15]G. Garbarino, A. Sow, P. Lejay, A. Sulpice, P. Toulemonde, M. Mezouar, and M. Nunez-Regueiro, Europhys. Lett. **86**, 27001 (2009).
[16]D. Braithwaite, B. Salce, G. Lapertot, F. Bourdarot, C. Marin, D. Aoki, and M. Hanfland, J. Phys.: Condens. Matter **21**, 232202 (2009).
[17]S. Medvedev, T. M. McQueen, I. A. Troyan, T. Palasyuk, M. I. Eremets, R. J. Cava, S. Naghavi, F. Casper, V. Ksenofontov, G. Wortmann, and C. Felser, Nature Mater. **8**, 630 (2009).
[18]S. Margadonna, Y. Takabayashi, Y. Ohishi, Y. Mizuguchi, Y. Takano, T. Kagayama, T. Nakagawa, M. Takata, and K. Prassides, Phys. Rev. B **80**, 064506 (2009).
[19]A. Subedi, L. Zhang, D. J. Singh, and M.-H. Du, Phys. Rev. B **78**, 134514 (2008).
[20]L. Zhang, D. J. Singh, and M.-H. Du, Phys. Rev. B **79**, 012506 (2009).
[21]W. Bao, Y. Qiu, Q. Huang, M. A. Green, P. Zajdel, M. R. Fitzsimmons, M. Zhernenkov, M. H. Fang, B. Qian, E. K. Vehstedt, J. H. Yang, H. M. Pham, L. Spinu, and Z. Q. Mao, Phys. Rev. Lett. **102**, 247001 (2009).
[22]S. Li, C. de la Cruz, Q. Huang, Y. Chen, J. W. Lynn, J. Hu, Y.-L. Huang, F.-C. Hsu, K.-W. Yeh, M.-K. Wu, and P. Dai, Phys. Rev. B **79**, 054503 (2009).
[23]F. Ma, W. Ji, J. Hu, Z.-Y. Lu, and T. Xiang, Phys. Rev. Lett. **102**, 177003 (2009).
[24]V. Tsurkan, J. Deisenhofer, A. Gunther, Ch. Kant, H.-A. Krug von Nidda, F. Schrettle, and A. Loidl, arXiv:1006.4453 v1 (2010).
[25]M. H. Fang, H. M. Pham, B. Qian, T. J. Liu, E. K. Vehstedt, Y. Liu, L. Spinu, and Z. Q. Mao, Phys. Rev. B **78**, 224503 (2008).
[26]F. Walz, J. Phys.: Condens. Matter **14**, R285 (2002).
[27]J. Yang, M. Mansui, M. Kawa, H. Ohta, C. Michioka, C. Dong, H. Wang, H. Yuan, M. Fang, and K. Yoshimura, J. Phys. Soc. Jpn. **79**, 074704 (2010).
[28]R. Viennois, E. Giannini, D. van der Marel, and R. Černý, J. Solid State Chem. (2010), in press.
[29]R. Hu, E. S. Bozin, J. B. Warren, and C. Petrovic, Phys. Rev. B **80**, 214514 (2009).
[30]S. Iikubo, M. Fujita, S. Niitaka, and H. Takagi, J. Phys. Soc. Jpn. **78**, 103704 (2009).
[31]K.-W. Lee, V. Pardo, and W. E. Pickett, Phys. Rev. B **78**, 174502 (2008).
[32]M.-J. Han and S. Y. Savrasov, Phys. Rev. Lett. **103**, 067001 (2009).
[33]Y. Ding, Y. Wang, and J. Ni, Solid State Commun. **149**, 505 (2009).
[34]S. Chadov, D. Scharf, G. H. Fecher, C. Felser, L. Zhang, and D. J. Singh, Phys. Rev. B **81**, 104523 (2010).
[35]J. M. Wills, O. Eriksson, M. Alouani, and D. L. Price, in: *Electronic Structure and Physical Properties of Solids: the Uses of the LMTO Method*, H. Dreysse (ed.), Springer Verlag, Berlin (2000), p. 148; M. Alouani and J. M. Wills, *ibid.*, p. 168; O. Eriksson and J. M. Wills, *ibid.* p. 247.
[36]G. E. Grechnev, R. Ahuja, and O. Eriksson, Phys. Rev. B **68**, 064414 (2003).
[37]U. von Barth and L. Hedin, J. Phys. C **5**, 1629 (1972).
[38]L. Nordström, O. Eriksson, M. S. S. Brooks, and B. Johansson, Phys. Rev. B **41**, 9111 (1990).
[39]A. V. Ruban, S. Khmelevskyi, P. Mohn, and B. Johansson, Phys. Rev. B **75**, 054402 (2007).

This article was published in English in the original Russian journal. Reproduced here with stylistic changes by AIP.